Annealing effect of platinum-incorporated nanowires created by focused ion/electron-beam-induced deposition*

Fang Jing-Yue(方靖岳)[a)†], Qin Shi-Qiao(秦石乔)[a)], Zhang Xue-Ao(张学骜)[a)], Liu Dong-Qing(刘东青)[b)], and Chang Sheng-Li(常胜利)[a)]

[a)] College of Science, National University of Defense Technology, Changsha 410073, China
[b)] College of Aerospace and Material Engineering, National University of Defense Technology, Changsha 410073, China

(Received 14 December 2013; revised manuscript received 10 March 2014; published online 10 June 2014)

Focused ion-beam-induced deposition (FIBID) and focused electron-beam-induced deposition (FEBID) are convenient and useful in nanodevice fabrication. Since the deposition is from the organometallic platinum precursor, the conductive lines directly written by focused ion-beam (FIB) and focused electron-beam (FEB) are carbon-rich materials. We discuss an alternative approach to enhancing the platinum content and improving the conductivity of the conductive leads produced by FIBID and FEBID, namely an annealing treatment. Annealing in pure oxygen at 500 °C for 30 min enhances the platinum content values from ∼18% to 30% and ∼ 50% to 90% of FIBID and FEBID, respectively. Moreover, we find that thin films will be formed in the FIBID and FEBID processes. The annealing treatment is helpful to avoid the current leakage caused by these thin films. A single electron transistor is fabricated by FEBID and the current–voltage curve shows the Coulomb blockade effect.

Keywords: electron-beam-induced deposition, ion-beam-induced deposition, annealing, current leakage, single electron transistor

PACS: 81.15.Jj, 68.35.Dv, 81.40.Ef **DOI:** 10.1088/1674-1056/23/8/088111

1. Introduction

Focused ion-beam-induced deposition (FIBID) and focused electron-beam-induced deposition (FEBID) are two promising techniques for nanoscaled rapid prototyping of micro- and nano-scaled patterns in laboratory.[1,2] The dual beam system can be employed to fabricate quantum dots or conductive lines at a chosen position in a nanodevice by the scanning electron microscope (SEM) operator in a few minutes. Thus, it provides opportunities in nanodevice fabrication.[3–8] The single electron transistor (SET) is one of the most investigated nanodevices in recent years.[9–13] The photolithography, electron-beam lithography (EBL), electron-beam evaporation, and lift-off procedures are commonly used techniques in SET production. As mentioned before, the dual beam system is a nano-lithography alternative, and some efforts have been made to investigate the SET using FIBID or FEBID techniques.[14,15] However, since the deposition in a dual beam system can be likened to a local CVD process, carbon-rich material rather than pure platinum will be deposited in the company of the decomposition of the organometallic gaseous precursor.[16–19] The low-purity is detrimental to the applications in writing conductive leads by FIBID and FEBID. In this work, we discuss the effect of annealing on the purifying of platinum incorporated depositions and the enhancing of their conductivities.

2. Experiment

The platinum depositions were produced on Si substrates with a 500-nm oxide layer by FIBID or FEBID. The substrates were sequentially cleaned in acetone, ethanol, and de-ionized water, and dried in ambient nitrogen . Subsequently, some FIBID samples, each with an area of 3 μm×3 μm, were produced on the silicon wafer in a dual beam system (FEI Helios Nanolab 600i) when the ion beam source voltage and current were set at 30 kV and 40 pA, respectively. The organometallic precursor $(CH_3)_3Pt(C_pCH_3)$ results in platinum-incorporated carbon-rich samples. After annealing at 500 °C for 30 min (heating rate of 10 °C·min^{-1}) in oxygen atmosphere (flux 30 sccm), the samples were cooled down to room temperature along with the cooling down of the furnace. Then, energy dispersive X-ray (EDX) analyses were performed to identify and characterize the elements of the samples, using HORIBA EMAX 7593-H in a field emission SEM (HITACHI S4800).

In order to measure the current–voltage (I–V) characteristics of platinum-incorporated wires created by FIBID and FEBID, pads on silicon wafers were first defined by photolithography and electron beam evaluation deposition (EBED). Afterwards, platinum-incorporated wires were pat-

*Project supported by the Research Project of National University of Defense Technology, China (Grant No. JC13-02-14) and the National Natural Science Foundation of China (Grant No. 11104349).

†Corresponding author. E-mail: fjy_nudt@yahoo.com.cn

© 2014 Chinese Physical Society and IOP Publishing Ltd

terned by the dual beam system. Some of them connected to the pads by a single wire, such as samples 1 and 2; some coupled the pads by a pair of wires with a narrow gap, such as samples 3 and 4. Then, the resistivity values of the wires were measured by a probe station (Wentworth PML 8000) and a semiconductor parametric analyzer (SPA) system (Agilent B1500A). By using the I/V sweep model of the SPA, electrical tests were done for the non-annealed and annealed samples. As for samples 1 and 2, we can obtain the resistivity values of the platinum-incorporated depositions and judge the influences of annealing, while the current leakage could be found in samples 3 and 4. Platinum-incorporated dots were deposited between the leads defined by electron beam lithography (EBL) and some SET devices were formed. After the annealing treatment, the *I*–*V* characteristics of the SET devices were measured in a liquid nitrogen Dewar by using Agilent B1500A.

3. Results and discussion

3.1. Improving the conductivity of platinum-containing nano-structures

The compositional changes of the thermally annealed FIBID and FEBID materials are investigated in order to apply these materials to the nano- and micro-electronic devices. After FIBID samples are produced on the silicon substrate, EDX analyses are taken to identify and characterize their elements. Figure 1 shows the EDS spectra before and after the annealing treatment. The measurement data are normalized after all of the elements have been analyzed twice. Compared with the sample without annealing, the sample after calcination is of much purer platinum; on the other hand, carbon and gallium are relatively removed. It can be confirmed that the atoms of carbon and oxygen react in the course of annealing, and the molecules of carbon dioxide escape along with the airflow.

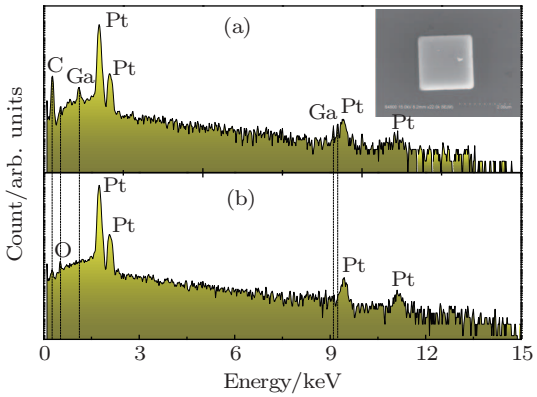


Fig. 1. (color online) EDX spectral data (a) before and (b) after annealing of a platinum-incorporated deposition by FEBID. The inset shows the SEM image of the sample.

To identify more exactly, some quantitative analyses are performed and the measurement data are shown in Table 1. The results show that the FIBID sample is a carbon-rich material with about 70% carbon atoms, while the platinum content is low and the atom percentage is less than 20%. With respect to the FEBID sample, the atomic concentrations of carbon and platinum are $\sim$ 90% and 6%, respectively. It is clear that the conductivity of the carbon-rich deposition will not be suitable for electron transfer in nanodevices. It is a disadvantage for the applications in nanoelectronics. However, the annealing treatment can enhance the platinum content to a certain extent. Due to the oxygenation at 500 °C, the carbon is apparently removed and the platinum content is increased. What is more, the element of oxygen is brought in to the material in the meantime. In addition, the enhancement of the platinum content is more remarkable in the FEBID sample than in the FIBID sample. We suppose that the smaller content of gallium and greater content of carbon is the main reason why FEBID samples can be purified more effectively than FIBID samples.

Table 1. The weights and atomic concentrations of the dual beam-induced resultants.

		FIBID				FEBID			
		C(K)	O(K)	Ga(L)	Pt(M)	C(K)	O(K)	Ga(L)	Pt(M)
Weight/%	No treatments	16.35	/	13.27	70.37	46.50	/	5.90	47.60
	Annealing	3.00	7.06	13.97	75.97	/	8.67	/	91.33
Atom/%	No treatments	71.18	/	9.96	18.86	92.18	/	2.01	5.81
	Annealing	19.50	34.44	15.65	30.41	/	53.65	/	46.35

Since some of the impurities are removed, the conductivity may be improved. Figure 2(a) shows the pads on a silicon wafer. There are ten sets of micro-electrodes. Each of them has three leads with gaps in between. Using one electrode as a common one, we can deposit two wires between them and form two subjects for our measurement. Figures 2(b) and (2c) show the samples 1 and 2, respectively. Sample 1 is produced by FIBID with the voltage and current of the ion beam source being 16 kV and 50 pA, respectively. Sample 2 is produced by FEBID with the voltage and current of the ion beam source being 20 kV and 1.4 nA, respectively. All of the wires are about 7 μm long; 1 μm and 50 nm wide for samples 1 and 2, respectively.

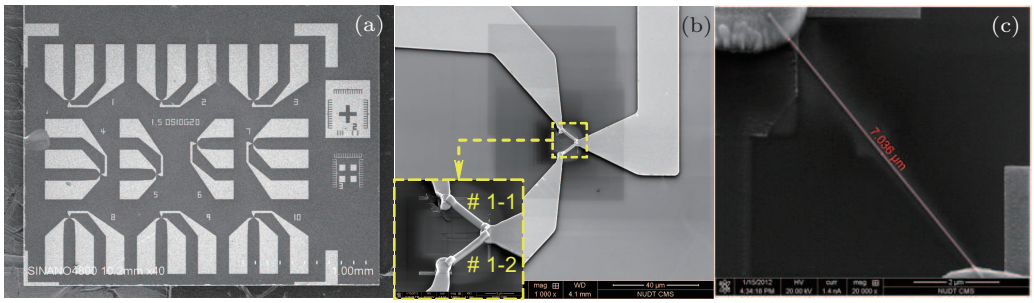


Fig. 2. (color online) SEM images of (a) a chip fabricated by using photolithography, (b) sample 1 with a set of electrodes in the chip when FIB-deposited platinum-incorporated wires are in contact with the leads, and (c) sample 2 with a platinum-incorporated nanowire produced by FEBID.

Figures 3(a) and 3(b) show the *I*–*V* currents of samples 1 and 2, respectively. An expected finding of conductivity improvement by annealing in sample 1 is evidenced, though the change is slight. However, sample 2 turnoff happens after annealing which doubts the positive effect of annealing on improving the conductive performance. To unambiguously assign the effect of annealing on the enhancing of FEBID sample conductivity, the results of some appendant experiments are shown in Fig. 4.

The structural changes of the thermally annealed FIBID and FEBID materials were investigated. Some nano-dots and a nano-line were deposited on a silicon substrate using FEB (Figs. 4(a) and 4(c)). Then, they were sent to a furnace to anneal at 200 °C for 30 min. After spontaneously cooling down to room temperature, they are measured by SEM, and the images are shown in Figs. 4(b) and 4(d). A collapse happens to the nano-dots during the annealing, and the nano-line breaks into many segments as a string of beads. In the oxidation, carbons go away and platinum atoms are redistributed from highly dispersed atoms to aggregated clusters and crystallize during the thermal annealing. It leads to a collapse of the FEBID sample. We suppose that the platinum atom redistribution of FEBID lines with finite dimension during the annealing is the main cause of the turnoff for sample 2. What is more, there is a noticeable phenomenon that a thin film, which could not be found before annealing, appears around the deposited dots or line after annealing. This thin film may do harm to a nanoscaled circuit, as it may destroy the insulation and cause current leakage between the leads.

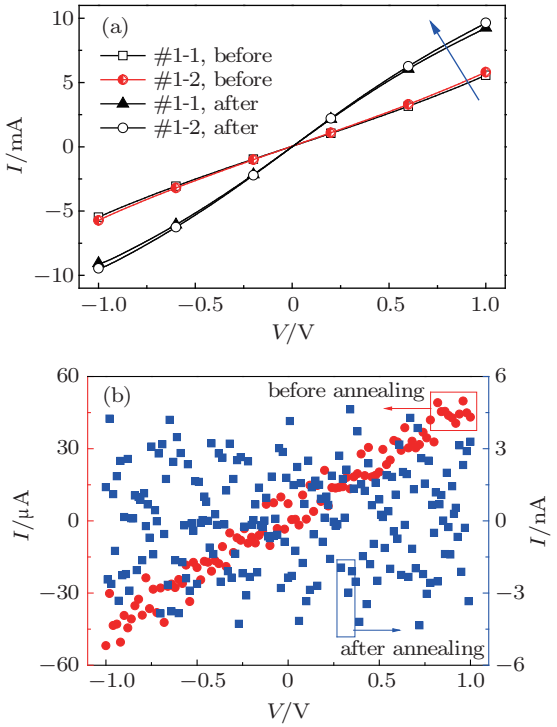


Fig. 3. (color online) The *I*–*V* characteristics of (a) FIBID sample 1 and (b) FEBID sample 2.

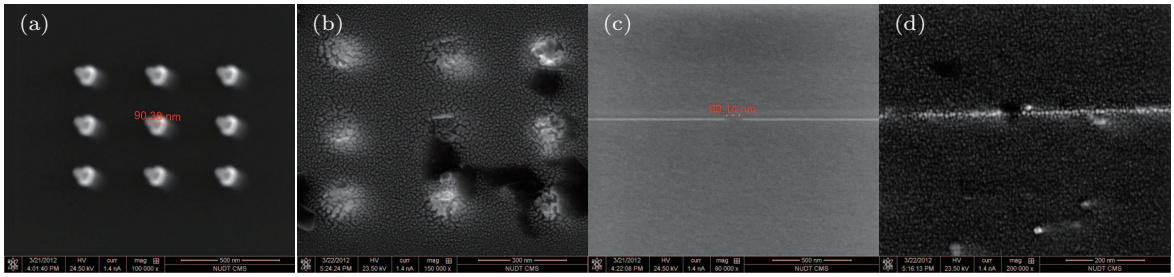


Fig. 4. (color online) SEM images of (a) nano-dots and (c) a nanoscaled line fabricated by FEBID, panels (b) and (d) are the corresponding resultants of panels (a) and (c) after annealing, respectively.

3.2. Sputtering effect of induced deposition

In order to investigate the thin film more exactly, we fabricate some couples of leads with narrow gaps. If a thin film is formed around the deposited leads, a current leakage can be measured through *I*–*V* tests. Figures 5(a) and 5(b) show the *I*–*V* characteristics of sample 3 produced by FEBID. The *I*–*V* curves show similar electron transfer mechanisms before and after annealing in Figs. 5(a) and 5(b). The nearly linear *I*–*V* curve implies that the resistance is about 100 kΩ before annealing. It is evident that thin films exist in the gaps between the FEBID leads and the linear *I*–*V* curves are of leaky current. After annealing the samples, the electron transfer mechanism changes into that of field emission. The thin films reveal their true features by annealing. Spontaneously, the thin films serving as bridges for electrons to transfer from one lead to the other, are destroyed. Thus, with the increase of the voltage, the electrons are stored in one lead in the beginning, when the potential barrier is changed, the stored electrons tunnel through the barrier as current exponentially increases.

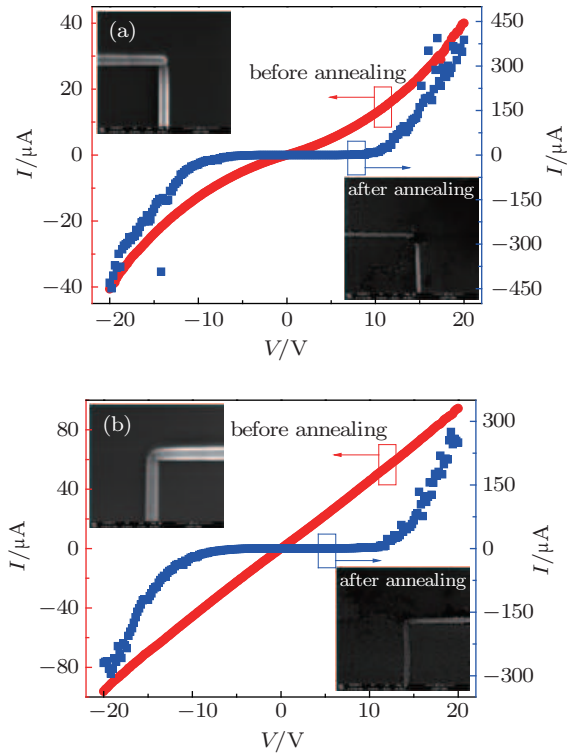


Fig. 5. (color online) The *I*–*V* characteristics of FEBID sample 3 before and after annealing. The insets show the FEBID leads with a narrow gap while the upper and lower insets are ones before and after annealing, respectively.

An electrical test is performed to verify that the thin films are also formed when FIBID leads are produced. Before annealing, the *I*–*V* curves are linear. After annealing, the electron transfer turns off in Fig. 6(a), however, the onset field emission is apparent in Fig. 6(b). In our opinion, the turnoff in Fig. 6(a) is just attributed to a wider gap between the leads than the one in Fig. 6(b). Thus, the arrival at the onset point of field emission is harder to achieve in Fig. 6(a) than in Fig. 6(b). Additionally, we find a tortuous channel in the lower inset of Fig. 6(a). In fact, the similar channels can be found for all of the couples of leads after annealing. It is of benefit to avoiding current leakage.

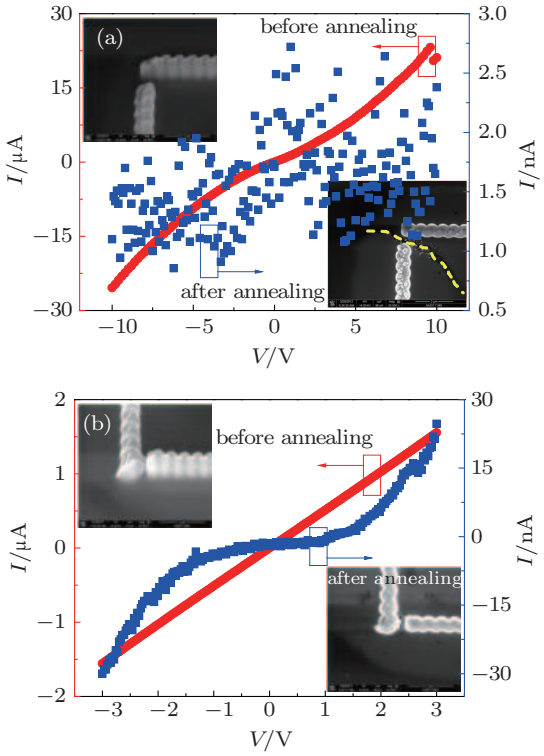


Fig. 6. (color online) The *I*–*V* characteristics of FIBID sample 4 before and after annealing. The insets show the FIBID leads with a narrow gap while the upper and lower insets are ones before and after annealing, respectively. The dashed line is a guide to the eyes.

3.3. Measurement of SET devices

Figure 7(a) shows the nano-scaled leads of a SET device. It is first fabricated by EBL and EBED, and then micro-scaled pads are produced and connected to the nano-leads by photolithography and EBED. The platinum-incorporated dot array is prepared by FEBID (Fig. 7(b)). After annealing at 200 °C for 30 min in oxygen, the *I*–*V* characteristics of the device are measured. Figure 8 shows the source–drain *I*–*V* curve and its corresponding differential conductance measured at 77 K. The *I*–*V* and *G*–*V* curves show that the device performs a Coulomb blockade effect. Though the collapse will happen to the platinum dot located in the source–drain gap during the annealing, making it separate into pieces of segments, one piece of the fragment may serve as a Coulomb island. Its charging energy is about 48 meV which can be obtained from the length of the low conductive region.[20,21]

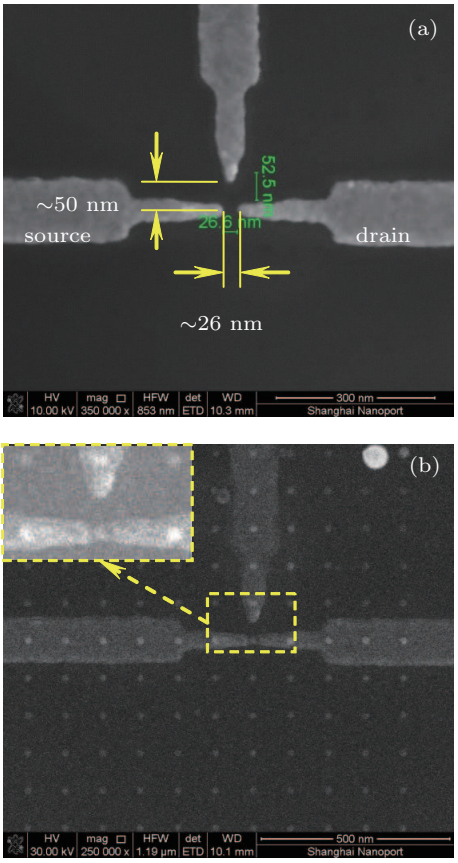


Fig. 7. (color online) SEM images of the electrodes (a) before and (b) after FEBID of the platinum dot array. The inset of panel (b) shows an enlarged core region. There is a platinum dot located in the source–drain gap.

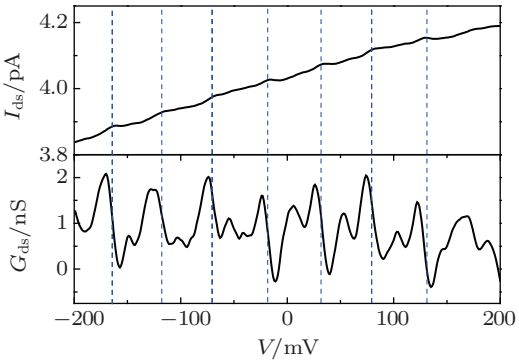


Fig. 8. The *I*–*V* curve and its corresponding differential conductance measured at 77 K with zero gate voltage.

4. Conclusions

In this paper, the effects of the thermal annealing of platinum-incorporated wires fabricated by FEBID and FIBID are investigated. By using the SPA and EDX spectrometer analyses, we find that the platinum content is increased and the carbon element is mostly removed, thus, the conductive properties are enhanced of the FEBID and FIBID samples by annealing post-treatment. What is more, we find that a thin film is formed during the induced deposition using FEB and FIB. The aggregated process and redistribution of platinum atoms during the annealing will break the thin film, making it separate into pieces of segments. Thus, the treatment of annealing is an alternative approach to avoid current leakage. Finally, SET devices are fabricated by FEBID with annealing treatments which show the Coulomb blockade effect.

Acknowledgement

Authors thank Chen Wen-Dy and Dr. Lin Ying-Hong, who are application engineers of FEI Company, for helpful discussions.

References

[1] Botman A, Mulders J J L, Weemaes R and Mentink S 2006 *Nanotechnology* **17** 3779
[2] Randolph S J, Fowlkes J D and Rack P D 2006 *Crit. Rev. Solid State Mater. Sci.* **31** 55
[3] Jafri S H M, Blom T, Wallner A, Welch K, StrΦmme M, Ottosson H and Leifer K 2011 *Microelectron. Eng.* **88** 2629
[4] Wu C H, Jhan F J, Chen J H, Jeng J T, Chen K L and Yang H C 2011 *IEEE Trans. Appl. Supercond.* **21** 375
[5] Li W X, Fenton J C, Gu C Z and Warburton P A 2011 *Microelectron. Eng.* **88** 2636
[6] Tseng A A 2005 *Small* **1** 924
[7] Zhang X A, Fang J Y, Sun J D, Qin H, Chang S L and Qin S Q 2013 *J. Nanosci. Nanotech.* **13** 2589
[8] Fang J Y, Qin S Q, Zhang X A, Wang F, Shao Z Z, Wang G and Chang S L 2013 *Microelectron. Eng.* **108** 1
[9] Su L N, Gu X F, Qin H and Yan D W 2013 *Acta Phys. Sin.* **62** 077301 (in Chinese)
[10] Zhang X G, Fang Z H, Chen K J, Qian X Y, Liu G Y, Xu J, Huang X F and He F 2011 *Acta Phys. Sin.* **60** 027304 (in Chinese)
[11] Li W, Xu L, Zhao W M, Ding H L, Ma Z Y, Xu J and Chen K J 2010 *Chin. Phys. B* **19** 047308
[12] Shen H H, Peng S M, Long X G, Zhou X S, Yang L, Liu J H, Sun Q Q and Zu X T 2012 *Chin. Phys. B* **21** 076101
[13] Ma Y Z, Pang L L, Zhu Y B, Wang Z G and Shen T L 2011 *Chin. Phys. B* **20** 078104
[14] Karre P S K, Bergstrom P L, Mallick G and Karna S P 2007 *J. Appl. Phys.* **102** 024316
[15] Cheam D D, Walczak K A, Archaya M, Friedrich C R and Bergstrom P L 2011 *Microelectron. Eng.* **88** 1906
[16] Botman A, Hesselberth M and Mulders J J L 2008 *Microelectron. Eng.* **85** 1139
[17] Cui Z 2005 *Micro-Nanofabrication Technologies and Applications* (Beijing: Higher Education Press) p. 144 (in Chinese) ISBN: 9787040263589
[18] Botman A, Mulders J J L, Weemaes R and Mentink S 2006 *Nanotechnology* **17** 3779
[19] Murakami K, Yamasaki N, Abo S, Wakaya F and Takai M 2005 *J. Vac. Sci. Technol. B* **23** 759
[20] David L K, Richard R, Andrew K L L, Alivisatos A P and Paul L M 1997 *Nature* **389** 699
[21] Choi B H, Hwang S W, Kim I G, Shin H C, Kim Y and Kim E K 1998 *Appl. Phys. Lett.* **73** 3129